The Effect of Thermo-Mechanical Treatments on $J_c(T, B)$ and T_{cs} of Nb-Ti Strands

Alexander K. Shikov, Victor I. Pantsyrny, Nina I. Kozlenkova, Liudmila V. Potanina, Roman M. Vasilyev, Igor N. Gubkin, Eugeniy V. Nikulenkov, Johann Emhofer, Michael Eisterer, and Harald W. Weber

***Abstract*—An extended database of critical current densities $J_c(T, B)$ and current sharing temperatures T_{cs} for Nb-Ti strands was obtained in this work. This data set allows one to make a more realistic forecast of the ITER poloidal field (PF) coil critical current at temperatures above 6 K and in a magnetic field of 6 T. It is found that $J_c(4.2\ \mathrm{K}, 5\ \mathrm{T})$ lies in the range from 700 to 2950 $\mathrm{A/mm^2}$, depending on the heat treatment regimes, and that $J_c(6.5\ \mathrm{K}, 6\ \mathrm{T})$ is 28 to 54 $\mathrm{A/mm^2}$ almost regardless of the applied heat treatment, i.e. the microstructure does not significantly affect $J_c(6.5\ \mathrm{K}, 6\ \mathrm{T})$ under such "extreme" conditions. It is shown, that $T_{cs}(6\ \mathrm{T})$ at a current of 31.2 A, which is close to the assumed operating current for the strand in the ITER PF1&6 coils, is 6.1–6.25 K. It is shown furthermore, that the application of multiparametric functions for the description of $J_c(T, B)$ or $V(I, T, B)$ leads to a reliable prediction of $J_c(T, B)$ only in a temperature and field range, where experimental data points are available (extrapolations result in large deviations).**

***Index Terms*—Critical current density, magnetic field, NbTi strand, temperature.**

I. Introduction

In accordance with the preliminary specification of the Nb-Ti strands for the PF conductors of the ITER magnet system a critical current density $J_c \geq 2900\ \mathrm{A/mm^2}$ (4.2 K, 5 T) was specified for all strands for different PF coils [1]. The main task concerned the problem of the temperature margin. The strands investigated at CEA (Bochvar, Alstom, and LMI), which met the ITER requirements of J_c at 4.2 K and $5\ \mathrm{T} \geq 2900\ \mathrm{A/mm^2}$), failed to meet the preliminary specified temperature margin $\Delta T = 1.5$ K by 0.2 to 0.3 K [2]. It was decided to investigate the $J_c(T)$ between 5 K and 6.5 K for Nb-Ti strands fabricated from the same initial materials, but with different heat treatments (HT), in order to evaluate the possibility of J_c optimization in this temperature range. An extended database on $J_c(T, B)$ for Nb-Ti strands over a wide temperature range enables more realistic predictions for the ITER PF coil performance and an adjustment of the operating parameters and the strand design.

II. $J_c(T, B)$ and $V(I, T, B)$ Parameterization

The Bottura formula [3] was used to describe $J_c(T, B)$:

$$J_c(T, B) = C_0 B^{-1}(1 - t^{1.7})^{\gamma} b^{\alpha}(1 - b)^{\beta}, \qquad (1)$$

where $t = T/T_c$, $b = B/B_{c2}(T)$ are the reduced temperature and field, respectively, and C_o, α, β, and γ are free parameters depending on the composition and the structure of the material. $B_{c2}(T)$ is described by (2), where $B_{c2}(0)$ is the upper critical field at $T = 0$ K:

$$B_2(T) = B_{c2}(0)(1 - t^{1.7}), \qquad (2)$$

The equation proposed in [4], [5] was used to describe $V(I)$:

$$V(I, T, B) = V_0 \exp\left(-\chi(1 - t)(1 - b)(1 - i)\right). \qquad (3)$$

Here $i = I/I_c(T, B)$ and $\chi = T_c(0)/T_0(0)$ is a fit parameter related to the broadening of the transition. The growth parameters for current $I_0(T, B)$, temperature $T_0(I, B)$ and magnetic field $B_0(I, T)$ were defined in [5].

III. Experimental

The PF type samples with a Cu/non Cu ratio of 1.6 were produced on the basis of the commercial grade Nb-47.5 $\pm$1 wt.% Ti alloy, using different HT regimes. Several intermediate HT were applied with the total duration from 60 to 240 hours at 350 °C, 380 °C and 400 °C. Totally cold worked samples were also prepared. The strand design with 4314 filaments was calculated on the basis of unified Cu/Nb/NbTi elements with a Cu/non Cu ratio of 0.43. At the final strand diameter of 0.73 mm filament diameter was 6.8 μm. In order to restore copper conductivity (RRR parameter) all the samples were subjected to additional anneal at 250°C for 1h at the final diameter. The study was also carried out on previously produced strand for PFCI (Poloidal Field Coil Insert) denoted as #1 with a Cu/non-Cu ratio of 1.4, filament number of 2346 and filament diameter of 9.98 μm. The details of samples fabrication are available in [6].

The measurements performed in VNIINM were described in more detail in [7]. At ATI, $V(I, B, T)$ was measured either in liquid helium or in helium gas flow. The maximal current available at 4.2 K was 300 A, but it was restricted to about 120 A in flowing helium gas due to thermal instabilities. A Cernox thermometer was used for temperature measurements. The critical current (I_c) was determined by an electric field criterion E_c of 10 $\mu\mathrm{V/m}$. J_c was calculated from $J_c = I_c/S$, where S denotes the cross sectional area of all Nb-Ti filaments. The critical temperature $T_c(B)$ and T_{cs} were determined by an electric field criterion E_c of 10 $\mu\mathrm{V/m}$. $V(T)$ characteristics were measured also by an inductive method at zero external field with a frequency of 10 kHz and an AC field amplitude of 0.3 mT. These measurements were carried out on the samples without copper matrix.

IV. Results and Discussion

A. $J_c(T, B)$ and $V(I, T, B)$

The experimental $J_c(T)$ at various B for the sample #21 are shown in Fig. 1. $J_c(T, B)$ obtained at VNIINM and ATI agree within 1–3% at 4.2 K and within ~10% at the level of 6.5 K.

Manuscript received August 26, 2008. First published June 30, 2009; current version published July 15, 2009.

A. K. Shikov, V. I. Pantsyrny, N. I. Kozlenkova, L. V. Potanina, R. M. Vasilyev, I. N. Gubkin and E. V. Nikulenkov are with the Bochvar Institute (VNIINM), Moscow, Russia (e-mail: vor@bochvar.ru).

J. Emhofer, M. Eisterer, and H. W. Weber are with the Atomic Institute of the Austrian Universities (ATI), Vienna, Austria (e-mail: eisterer@ati.ac.at).

Digital Object Identifier 10.1109/TASC.2009.2019134

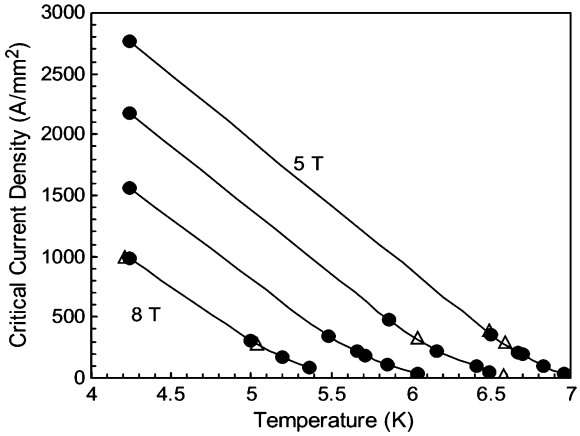

Fig. 1. Critical current density as a function of temperature at 5 T, 6 T, 7 T, and 8 T for the strand #21. The full symbols refer to VNIINM data, the triangles represent I_c measured at ATI. The solid lines were generated using (1) and the parameters of the first row of Table I.

TABLE I
FIT PARAMETERS OBTAINED BY PROCESSING THE $I_c(T, B)$ AND $V(I, T, B)$ DATA MEASURED AT VNIINM AND ATI FOR THE STRAND #21

	χ	C_0 (A·T)	$B_{c2}(0)$ (T)	T_c (K)	α	β	γ	mean relative error
I_c (VNIINM)	-	47142 ±18993	14.11 ±0.49	9.23 ±0.10	1.52 ±0.33	1.59 ±0.33	2.90 ±0.33	21.8 %
I_c (ATI)	-	223728 ±192440	15.38 ±0.31	9.03 ±0.03	3.17 ±0.85	2.70 ±0.52	2.25 ±0.09	15.3 %
I_c (ATI) + 4.2 K, 5 and 6T		55787 ±11032	14.92 ±0.19	9.03 ±0.04	1.69 ±0.15	1.91 ±0.15	2.23 ±0.10	24 %
I_c (VNIINM) - 4.2K, 5 and 6T	-	668163 ± 3652752	15.52 ±1.57	9.19 ±0.15	3.94 ±5.98	3.38 ±3.21	2.63 ±0.70	18.1 %
I_c (VNIINM) 4.2K - 6 K	-	26801 ±13146	13.91 ± .97	9.01 ±0.41	1.19 ±0.39	1.26 ±0.40	2.41 ±1.08	3.9 %
$V(I, T, B)$ full	183 ±4	112778 ±5790	15.01 ±0.05	9.10 ±0.01	2.42 ±0.16	2.30 ±0.08	2.31 ±0.02	4.1 %

Table I represents fit parameters obtained by processing $I_c(T, B)$ (rows 1–5) and $V(I, T, B)$ (row 6) data. A comparison of the parameters in rows 1 and 2 (Table I) shows that despite the good agreement between the experimental data sets, the discrepancy of the fit parameters describing both data sets is considerable.

Fig. 2 presents $J_c(T)$ at 5 T and 6 T measured at VNIINM and ATI as well as $J_c(T)$ calculated with the parameters of Table I. The ATI fit parameters describe the ATI data set rather well, but these parameters cannot be used for the extrapolation of $J_c(T, B)$ to low temperatures and low magnetic fields, i.e. outside the experimental area. Also the fit parameters obtained from the VNIINM data set without $J_c(4.2\,\mathrm{K}, 5\,\mathrm{T})$ and $J_c(4.2\,\mathrm{K}, 6\,\mathrm{T})$ cannot be used for a prediction of J_c at low fields and low temperatures (Fig. 2).

In exactly the same way the parameters obtained by processing of $J_c(T, B)$ data set without experimental points for temperatures above 6 K (row 5 of Table I) cannot be used for the extrapolation of $J_c(T, B)$ to high temperatures. As an example experimental points $J_c(6\,\mathrm{T}, T)$ and the curve calculated using (1) and the parameters of the row 5 of Table I are presented on the inset in Fig. 2.

These results indicate, that the area in which a reliable prediction can be made, is limited to the range of experimental points. The I_c prediction beyond the experimental area can result in large errors when applying this multiparametric description.

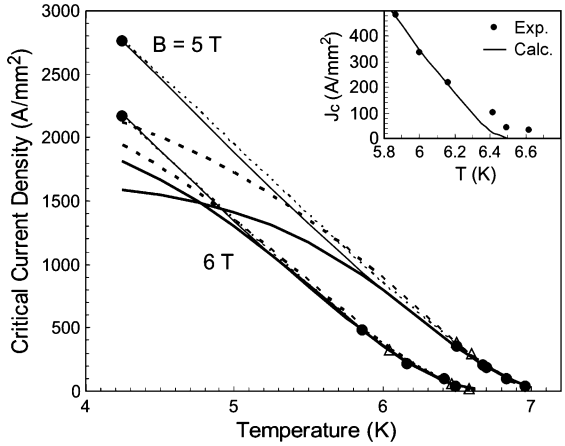

Fig. 2. Critical current density as a function of temperature at 5 T and 6 T for the strand #21. The open circles refer to the VNIINM data, the dark triangles to the ATI data. Thin solid, thick dotted, thin dotted and thick solid lines are calculated using (1) and the parameters of the first, second, third, and fourth row of Table I, respectively. The inset shows experimental points for 6 T and the curve calculated using (1) and the parameters of the fifth row of Table I.

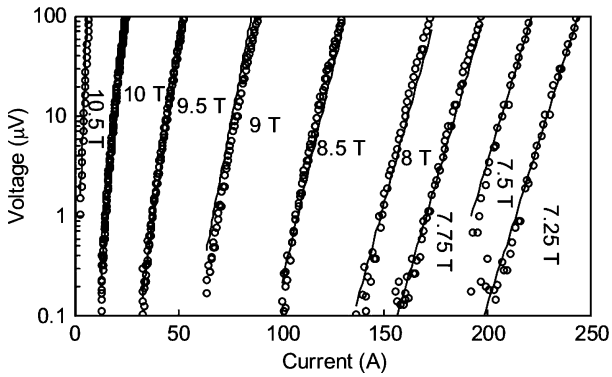

Fig. 3. Experimental and calculated $V(I)$ characteristics for the strand #21V at various B at 4.2 K. The solid lines are calculated using (3) and the parameters given in row 5 of Table I.

Some of the experimental and calculated $V(I)$ characteristics for the sample #21 are presented in Fig. 3. The corresponding fit parameters obtained by processing of $I_c(T, B)$ and $V(I, T, B)$ data are presented in rows 2 and 6 of Table I respectively. Note that the parameterization made on the basis of the $V(I)$ data set increases significantly the accuracy of the fit parameters determination compared to the parameterization based on the $I_c(T, B)$ data set.

B. Effect of Final Strain and Heat Treatment on $J_c(T, B)$

The effect of the final drawing (FD) and HT on J_c and the scaling parameters is presented in Table II. The cold worked sample #01 is characterized by low values of the α and β coefficients because this sample has a completely different structure than heat treated samples. Fig. 4 shows $J_c(T, 6\,\mathrm{T})$ of the samples studied at ATI and VNIINM. Letter V indicates data measured in ATI. One can see a good agreement between data measured at ATI and VNIINM at high temperatures. $J_c(6.5\,\mathrm{K}, 6\,\mathrm{T})$ lies in the range from 28 to 54 $\mathrm{A/mm^2}$. The specified operation current density, 196 $\mathrm{A/mm^2}$ [1], is achieved at T_{cs} values from 6.15 K to 6.25 K at 6 T in all samples, except for the cold worked one (#01).

Fig. 5 shows $J_c(4.2\ \mathrm{K}, B)$ of several samples. Similar $J_c(4.2\ \mathrm{K}, B)$ were obtained previously in [8]. It should be noted that all heat treatments applied with the purpose to

TABLE II
EFFECT OF FINAL STRAIN AND HEAT TREATMENT ON $J_c(4.2\ \mathrm{K}, 5\ \mathrm{T})$, $J_c(6.5\ \mathrm{K}, 6\ \mathrm{T})$, AND FITTING PARAMETERS

Sample	T(°C)/ t (h)	Final Drawing	J_c(4K,5T) (A/mm^2)	J_c(6.5K,6T) (A/mm^2)	C_0 (A·T/mm^2)	$B_{c2}(0)$ (T)	T_c (K)	α	β	γ
#01	-	3470	705	40	31809	14.8	9.0	1.3	1.0	2.2
#41	380/120	26	2749	30	260874	14.52	9.01	1.43	1.53	2.77
#21	380/120	64	2799	44	290820	14.11	9.23	1.52	1.59	2.90
#61	380/200	70	2911	54	603550	14.81	9.20	2.14	2.16	2.56
#1	385/120	64	2932	20	400199	14.74	9.03	1.73	1.88	2.53
#81	380/200	57	2826	28	519504	14.9	9.01	2.0	2.1	2.4
#71	380/200	64	2876	28	633392	15.2	8.93	2.13	2.28	2.21
#51	380/200	84	2800	29	330330	14.62	8.98	1.67	1.77	2.39
#310	350/60	70	2017	32	290062	15.19	8.88	2.10	1.79	2.17
#312	350/60	57	2000	28	518530	15.41	8.88	2.56	2.09	2.14

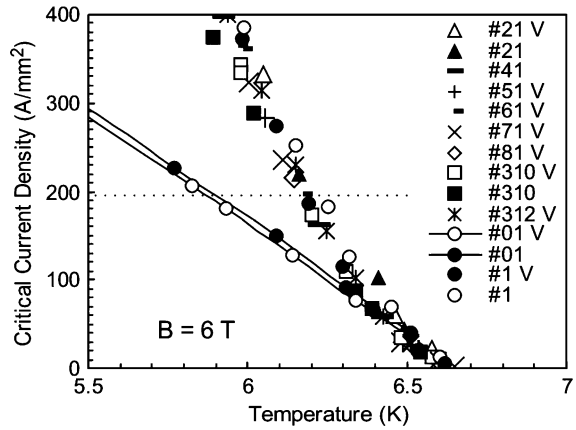

Fig. 4. Critical current density as a function of temperature at 6 T. "V" indicates data measured at ATI. The dotted line specifies the operational current density for the ITER PF coils.

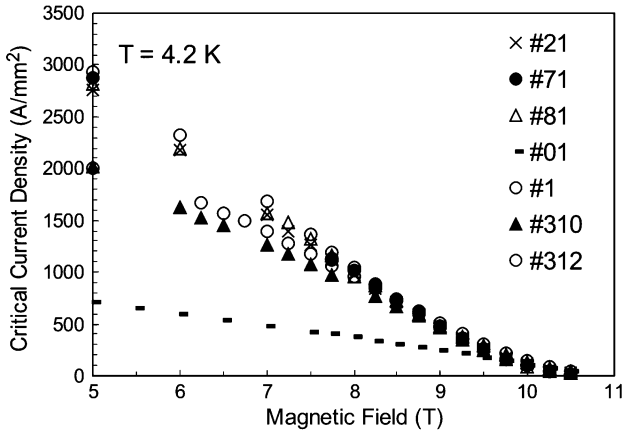

Fig. 5. Critical current density as a function of magnetic field at 4.2 K for different strands.

change the filaments' microstructure did not significantly affect $J_c(6.5\ \mathrm{K}, 6\ \mathrm{T})$ or $J_c(4.2\ \mathrm{K}, B > 9.5\ \mathrm{T})$. The critical current density does not correlate with the microstructure in the same way at such ultimate conditions for Nb-Ti conductors (high T and B) as under "usual" operating conditions (2 to 5 K, 3 to 6 T).

TABLE III
PARAMETERS χ AND T_0 FOR THE SAMPLE #21

	$V(T)$ I=0.4A	$V(T)$ I = 31.2 A	$V(I)$ (T > 6 K)	$V(I)$ (T > 4.2 K)	$V(I)$ (4.2 K)
χ	409	-	278	219	212
T_0	0.022	0.023	0.033	0.042	0.043

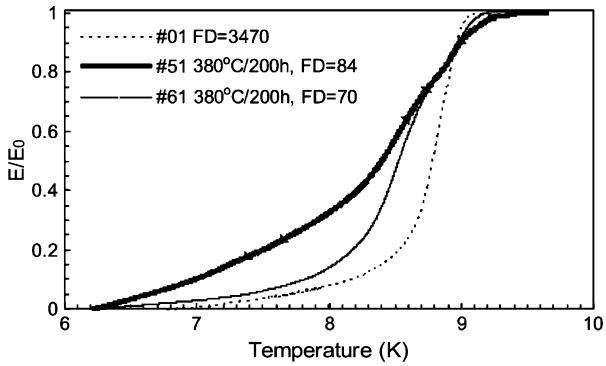

Fig. 6. AC normalized permeability as a function of temperature for the cold worked (#01) and heat treated (#51, #61) samples.

C. $V(T)$ Characteristics

$V(T)$ was measured at fixed magnetic field with an applied current of 0.43 A and 31.2 A ($J_{op} = 196\ \mathrm{A/mm^2}$). T_0 was obtained from $V(T)$ and from $V(I)$. The parameter T_0 determined from $V(T)$ at 0.43 A is in the range from 0.02 K to 0.028 K for heat treated samples. For the sample #21 $T_0(0.4\ \mathrm{A})$ is 0.022 K and does not depend on magnetic field up to 9 T within experimental error. $T_0(31.2\ \mathrm{A})$ for the sample #21 is equal to 0.023 K. For the cold worked sample #01 $T_0 = 0.01$ K. T_0 was determined also from $V(I)$ with (4) [5]. In the range of temperatures and magnetic fields, where $I_c(T, B)$ is nearly linear we have:

$$T_0 = I_0/(dI_c/dT). \tag{4}$$

Table III presents χ and T_0 obtained from $V(T)$ and from the evaluation of the $V(I)$ characteristics at various temperatures.

At temperatures below ~6 K, the sample is characterized approximately by the same χ and T_0, while T_0 decreases at high temperatures. Thus, with increasing current (decreasing temperature) some current redistribution occurs in the sample, which leads to an increase of T_0. On the basis of these results we propose that the higher homogeneity of the samples (lower T_0 values) at high temperatures is caused by the transition of "lower-T_c" components in the Nb-Ti filaments into the normal state. The AC measurements of the $V(T)$ revealed a noticeable inhomogeneity of the NbTi samples under study. Fig. 6 shows that the cold worked sample #01 is the most homogeneous concerning structure and composition. The HT changes the shape of the transition measured by the inductive method. The larger final cold deformation of heat treated samples also results in a slight broadening of the AC transition.

According to [9] up to 17–20% of filaments volume is occupied by α-Ti precipitates which form due to solid solution decomposition during a HT of a sample made on the basis of Nb-47.8 wt.% Ti alloy. As evident from [10], in process of HT Nb-Ti matrix is depleted in Ti to a level 37 wt.% to 38 wt.%.

The local composition in the superconducting filaments may vary significantly and differ from the initial one. Very likely, the broadening of the inductive transition indicates a re-solution of small sized particles of α-Ti precipitate into the solid solution

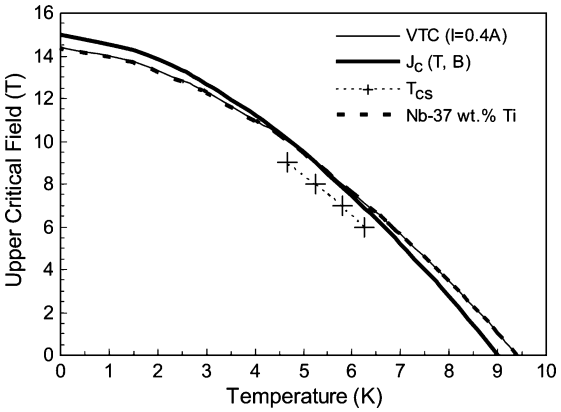

Fig. 7. Upper critical field as a function of temperature for the sample #1. The dashed line is calculated using (2) and literature data for $T_c(0)$ and $B_{c2}(0)$. The crosses represent T_{cs} at various magnetic fields.

with increasing deformation. However, no correlation between the transition width and $J_c(4.2\ \mathrm{K}, 5\ \mathrm{T})$ or $J_c(6.5\ \mathrm{K}, 6\ \mathrm{T})$ was observed.

It is of interest to examine the upper critical field $B_{c2}(T)$. Fig. 7 shows $B_{c2}(T)$ of the sample #1. The data represent results of $T_c(B)$ measured with an applied current of 0.43 A (the curve is denoted as VTC in Fig. 7). $T_c(0)$ obtained from VTC measurements was 9.4 K and $B_{c2}^{WHH}(0)$ was 14.37 T. $B_{c2}^{WHH}(0)$ was obtained from the following equation:

$$B_{c2}^{WHH}(0) = -0.69 \cdot T_c \cdot (dB_{c2}/dT). \tag{5}$$

$B_{c2}(T)$ was also calculated from (2) using $B_{c2}(0)$ and $T_c(0)$ obtained from fitting the $J_c(T, B)$ data (shown in Fig. 7 as thick solid line and denoted as $J_c(T, B)$). The $B_{c2}(T)$ curve, which is obtained from $V(T)$ measured at low currents, characterizes the current path with the highest T_c, whereas the $B_{c2}(T)$ curve obtained from the $J_c(T, B)$ data set characterizes those parts of the NbTi filaments carrying most of the currents. The difference of these two curves denotes some inhomogeneity of superconductor.

Fig. 7 also presents the $B_{c2}(T)$ dependence of the Nb-37 wt.% Ti solid solution which was calculated from (2). $T_c(0) = 9.5\ \mathrm{K}$ and $B_{c2}(0) = 14.5\ \mathrm{T}$ for Nb-37 wt.% Ti were taken from [10]–[13]. Because of the rather large scatter of these data in literature, the $B_{c2}(T)$ dependence of the Nb-37 wt.% Ti solid solution is only a qualitative indication. The part of the material containing 37 wt.% Ti has $B_{c2}(T)$ lying very close to the curve denoted by VTC and above $B_{c2}(T)$ constructed on the basis of $J_c(T, B)$ data.

The $T_{cs}(\mathrm{B})$ dependence measured with a current of 31.2 A is also presented in Fig. 7. The point (6.5 K; 6 T) required in the preliminary ITER specification lies slightly above the $T_{cs}(31.2\ \mathrm{A}, B)$ curve.

On the basis of all the results obtained we conclude that in inhomogeneous materials containing regions of different composition with different $T_c(0)$ and $B_{c2}(0)$, the reduction in cross section of the superconducting paths proves to be more important for $J_c(6.5\ \mathrm{K}, 6\ \mathrm{T})$ than the microstructure. As a result, both cold-worked and heat treated samples have approximately equal J_c at high temperature and high magnetic field, in particular, at 6 T above 6.3 K (see Fig. 4).

V. Summary

Nb-Ti wires were fabricated using various regimes of HT (from totally cold drawn to heat treated for 60 to 240 hours at 350, 380, and 400°C). The comparison of experimental $J_c(T, B)$ data from VNIINM and ATI showed very good agreement. We have shown that the application of multiparametric functions for $J_c(T, B)$ or $V(I, T, B)$ processing leads to a reliable prediction of $J_c(T, B)$ only in a temperature and field range, where experimental points are available. Using the experimental $V(I, T, B)$ data for the parameterization instead of the $J_c(T, B)$ data improves the accuracy of the obtained fit parameters by a factor of $\sim$4. $J_c(4.2\ \mathrm{K}, 5\ \mathrm{T})$ lies in the range from 700 to 2950 $\mathrm{A/mm^2}$ depending on the heat treatment applied. $J_c(6.5\ \mathrm{K}, 6\ \mathrm{T})$ is 28 to 54 $\mathrm{A/mm^2}$, regardless of the heat treatment, i.e. the microstructure does not significantly affect $J_c(6.5\ \mathrm{K}, 6\ \mathrm{T})$ under such "extreme" conditions. The results confirm that the requirement for $J_c(6.5\ \mathrm{K}, 6\ \mathrm{T})$ in the preliminary ITER design specification is not achievable in NbTi. $T_{cs}(6\ \mathrm{T})$ at a current of 31.2 A, which is close to the assumed operating current for the strand in the ITER PF1&6 coils, was found to be 6.1 to 6.25 K. The temperature margin to 5 K is lower than specified for the PF1&6 coils (1.5 K). The results of this study enable more realistic predictions of the ITER PF coil performance. The tests of PFCI, which were conducted at JAEA (Japan) in June 2008, completely confirmed the results of this study—T_{cs} found there was 6.22 K at 45 kA and 6 T [14].

References

[1] [Online]. Available: www.iter.org/pdfs/PDD2-1.pdf

[2] L. Zani, E. Mossang, M. Tena, J.-P. Serries, and H. Cloez, "$J_c(B, T)$ characterization of NbTi Strands used in ITER PF-relevant insert and full-scale samples," *IEEE Trans. Appl. Supercon.*, vol. 15, no. 2, pp. 3506–3509, 2005.

[3] L. Bottura, "A practical fit for the critical surface of NbTi," *IEEE Trans. Appl. Supercond.*, vol. 10, no. 1, pp. 1054–1057, 2000.

[4] N. Fogel and A. Sidorenko, "Scaling behavior of resistive transitions in thin superconducting films," *Phys. Lett. A*, vol. 68, no. 5/7, pp. 465–458, 1978.

[5] N. Kozlenkova, V. Pantsyrnyi, A. Shikov, A. Vorobieva, and A. Mitin, "Scaling of the $V(I)$ characteristics in the ITER type $\mathrm{Nb_3Sn}$ strands in relation to the applied field and temperature," *IEEE Trans. Appl. Supercon.*, vol. 15, no. 2, pp. 3450–3453, 2005.

[6] H. W. Weber *et al.*, "Analysis of PF Conductor With High Cu/non-Cu Ratio," Transl.: Association EURATOM-OeAW, Atominstitute, Wien, Austria, , Oct. 2007, Final Report to Technology Task TW5-TMSC-PFANAL (Contract No 05-1326).

[7] N. Kozlenkova, G. Vedernikov, A. Shikov, L. Potanina, A. Filatov, A. Vorobieva, V. Pantsyrnyi, and I. Gubkin, "Study on $I_c(T, B)$ for the NbTi strand intended for ITER PF insert coil," *IEEE Trans. Appl. Supercond.*, vol. 14, no. 2, pp. 1028–1030, 2004.

[8] P. J. Lee and D. C. Larbalestier, "An examination of the properties of SSC phase II R&D strands," *IEEE Trans. Appl. Supercon.*, vol. 3, no. 1, pp. 833–841, 1993.

[9] P. J. Lee and D. C. Larbalestier, "Development of nanometer scale structures in composites of Nb-Ti and their effect on the superconducting critical current density," *Acta Metall.*, vol. 35, no. 10, pp. 2523–2536, 1987.

[10] P. Lee, "Abridged metallurgy of ductile alloy superconductors," in *Willey Encyclopedia of Electrical and Electronics Engineering*, J. G. Webster, Ed. New York: Wiley, 1999, vol. 21, pp. 75–87.

[11] I. E. Leksina, G. P. Motulevich, A. A. Shubin, I. A. Baranov, V. A. Sitnikov, and V. S. Shmulevich, "The optical properties of superconducting alloy NbTi," *FMM*, vol. 29, no. 1, pp. 97–107, 1970.

[12] C. Meingast, P. J. Lee, and D. C. Larbalestier, "Quantitative description of a high J_c Nb-Ti superconductor during its final optimization: I. Microstructure, T_c, H_{c2}, and resistivity," *J. Appl. Phys.*, vol. 66, no. 12, pp. 5962–5970, 1989.

[13] L. Miu, D. Niculescu, and E. Cruceanu, "The effect of precipitation heat treatments on the critical temperature in Ti- rich Nb-Ti alloys," *J. Mater. Science Lett.*, vol. 2, pp. 425–427, 1983.

[14] L. Bottura, private communication.